Endonuclease FEN1 coregulates ERα activity and provides a novel drug interface in tamoxifen resistant breast cancer

Running Title: Endonuclease FEN1 coregulates ERα activity.

Koen D. Flach[1,2,10], Manikandan Periyasamy[3], Ajit Jadhav[4], Dorjbal Dorjsuren[4], Joseph C. Siefert[1,2], Theresa E. Hickey[5], Mark Opdam[6], Hetal Patel[3], Sander V. Canisius[7], David Wilson III[8], Maria Donaldson Collier[1,2], Stefan Prekovic[1,2], Marja Nieuwland[9], Roelof J. Kluin[9], Alexey Zakharov[4], Jelle Wesseling[6], Lodewyk F.A. Wessels[2,7], Sabine C. Linn[6], Wayne D. Tilley[5], Anton Simeonov[4], Simak Ali[3], Wilbert Zwart[1,2,11*]

Affiliations:

[1]Department of Oncogenomics, [6]Department of Molecular Pathology, [7]Department of Molecular Carcinogenesis, [9]Genomics Core Facility, [10]Division of Gene Regulation, The Netherlands Cancer Institute, 1066 CX Amsterdam, The Netherlands.

[2]Oncode Institute, the Netherlands

[3]Department of Surgery and Cancer, Imperial College London, Hammersmith Hospital Campus, Du Cane Road, London W12 0NN, UK.

[4]National Center for Advancing Translational Sciences, National Institutes of Health, 9800 Medical Center Drive, MSC 3370, MD 20892, United States.

[5]Dame Roma Mitchell Cancer Research Laboratories, Adelaide Medical School, Faculty of Health Sciences, DX Number 650 801, University of Adelaide, Adelaide, South Australia 5005, Australia.

[8]Laboratory of Molecular Gerontology, Intramural Research Program, National Institute on Aging, National Institutes of Health, Bayview Blvd 251, Baltimore, MD 21224, United States.

[11]Laboratory of Chemical Biology and Institute for Complex Molecular Systems, Department of Biomedical Engineering, Eindhoven Universtity of Technology, Eindhoven, The Netherlands

[*]To whom correspondence should be addressed: Wilbert Zwart, w.zwart@nki.nl, +31205122101

Funding

This work was supported by the Dutch Cancer Society KWF, Netherlands Organisation for Scientific Research (NWO), A Sister's Hope, the National Center for Advancing Translational Sciences, National Institutes of Health [R03 MH092154-01], National Institute on Aging, the National Health and Medical Research Council of Australia [ID 1084416; ID 20160711 to WDT and THE], the Royal Adelaide Hospital Research Foundation and the Cancer Australia / National Breast Cancer Foundation [ID CA1043497].

Conflict of interest

The authors report no conflict of interest.

Abstract: Estrogen receptor α (ERα) is a key transcriptional regulator in the majority of breast cancers. ERα-positive patients are frequently treated with tamoxifen, but resistance is common. In this study, we refined a previously identified 111-gene outcome prediction-classifier, revealing FEN1 as the strongest determining factor in ERα-positive patient prognostication. FEN1 levels were predictive of outcome in tamoxifen-treated patients, and FEN1played a causal role in ERα-driven cell growth. FEN1 impacted the transcriptional-activity of ERα by facilitating coactivator recruitment to the ERα transcriptional complex. FEN1 blockade induced proteasome-mediated degradation of activated ERα, resulting in loss of ERα-driven gene expression and eradicated tumor cell proliferation. Finally, a high-throughput 465,195 compound screen identified a novel FEN1 inhibitor, which effectively blocked ERα-function and inhibited proliferation of tamoxifen-resistant cell lines as well as ex-vivo cultured ERα-positive breast tumors. Collectively, these results provide therapeutic proof-of-principle for FEN1 blockade in tamoxifen-resistant breast cancer.

Significance: Findings show that pharmacological inhibition of FEN1, which is predictive of outcome in tamoxifen-treated patients, effectively blocks ERα function and inhibits proliferation of tamoxifen-resistant tumor cells.

Introduction

Approximately 70% of all breast tumors are of the luminal subtype and their proliferation often depends on the activity of estrogen receptor α (ERα). Following ERα activation by estradiol (E2), a transcriptional complex is formed, initiated by Steroid Receptor Co-activator (SRC) p160 recruitment, driving ERα-mediated transcription and cell proliferation programs (1).

Tamoxifen is often used in ERα–positive breast cancer patients, where it competitively blocks E2-binding, preventing co-activator-binding pocket formation and inhibiting cell proliferation (2). P160 member SRC3 (NCOA3, AIB1) is frequently amplified in breast tumors and correlates with a poor outcome after tamoxifen treatment (3).

Previously, we assessed the genome-wide chromatin binding landscape of all three p160 coactivators in MCF-7 breast cancer cells (4). Preferentially-enriched chromatin binding sites for each of the p160 family members were found, where genomic regions preferentially bound by SRC3 were uncovered proximal to 111 E2-responsive genes. Based on these genes, we developed a prognostic classifier for outcome after tamoxifen treatment. Which individual genes in the original classifier are critically involved in the observed clinical outcome remains elusive.

Besides recruitment of classic coregulators such as p160 proteins, DNA-modulating and DNA repair factors can also be recruited by ERα (5), as recently shown for APOBEC3B (6). APOBEC3B induces C-to-U deamination at ERα binding regions, leading to uracil DNA glycosylase (UNG) recruitment and ultimately to phosphorylation of H2AX at Serine 139 (γH2AX) (6). While in theory the resulting UNG-mediated region of DNA -that contains neither a purine nor a pyrimidine (abasic site)- can be repaired by the Base Excision Repair (BER) pathway (7), the exact interplay of BER proteins with ERα function remains unclear.

FEN1 is a member of the RAD2 nuclease family and cleaves overhanging flap structures that arise during lagging-strand DNA synthesis (e.g. Okazaki fragments) (8) or long-patch BER, yielding a single-stranded DNA nick which can be ligated by DNA-ligase 1 (LIG1) (7). FEN1 deficiency predisposes to tumor development and FEN1 is upregulated in numerous tumor types, including breast cancer (9). Although endogenous ERα/FEN1 interactions have not been reported, incubation of immobilized FLAG-tagged ERα with MCF-7 nuclear extracts did identify FEN1 as an ERα-associating protein (10). Even though endogenous FEN1 was described as recruited to the TFF1 promoter and FEN1 knockdown resulted in reduced TFF1 mRNA expression (10), it remains unknown whether FEN1 regulates estrogen responsiveness in a genome wide manner or by which mechanism. Additionally, FEN1 levels correlate negatively with overall survival in breast cancer patients (11), but whether ERα-status is the driving force behind this clinical observation remains unclear.

Here, we demonstrate that FEN1 dictates the transcriptional activity of ERα by facilitating the formation of a functional transcriptional complex. Perturbation of FEN1 function results in deregulated ERα-responsive gene expression and reduced cell proliferation. FEN1 additionally regulates ERα's activity by stabilizing chromatin interactions after activation. We show that FEN1 is a predictive marker of tamoxifen response in ERα-positive breast cancer patients, playing a key role in ERα-driven cell proliferation. A novel small molecule inhibitor of FEN1 blocked proliferation of tamoxifen resistant cell lines as well as primary ERα-positive tumor explants, yielding a novel therapeutic lead in the clinical management of tamoxifen resistance. Cumulatively, we present a pioneering proof-of-concept that spans from gene classifier and causal gene identification, to molecular mechanism, novel drug development and validation in ERα-positive breast cancer.

Materials and Methods

Colony formation

For the colony formation assay 2500 cells/well were plated in 48-well format in appropriate culture medium. After attachment of cells to the bottom of the well, the FEN1 inhibitor was administered and when appropriate 100 nM 4OH-tamoxifen was added. After 7 days cells were fixed with 100% of methanol and cells were stained with 0.2% crystal violet. For quantification the crystal violet was dissolved in 10% acetic acid and the optical density was measured at 560 nm.

Cell culture

MCF-7, T47D, MDA-MB-231, CAL120 cells were cultured in DMEM medium in the presence of 10% FBS and antibiotics (penicillin, streptavidin). TAMR and MCF7-T cells were cultured in phenol-red-free DMEM containing 5% charcoal-treated serum (CTS; HyClone), 2 mmol/L of L-glutamine, antibiotics and 100 nM 4OH-tamoxifen. BT20 cells were cultured in MEM in the presence of 10% FBS and antibiotics. For hormone deficient conditions, cells were deprived of hormone for 72 hours, by culturing in phenol-red-free DMEM containing 5% charcoal-treated serum, antibiotics and supplemented with L-glutamine, prior to hormone treatment. Hormone treatments consisted of solvent Dimethylsulfoxide **(**DMSO), 10 nM of estradiol, 100 nM of 4OH-tamoxifen or 100 nM of fulvestrant. All cell lines were tested for mycoplasma every 3 months and were genotyped for authenticity by Applied Biosystems®. MCF-7, T47D and MDA-MB-231 were purchased from ATCC. CAL120 and BT20 cells were kindly provided by R.L. Beijersbergen. MCF7-T and TAMR (tamoxifen resistant MCF-7 derivatives (45,46) were kindly provided by Kenneth P. Nephew and R.I Nicholson.

RNA-seq

Cells transfected with siFEN1 or siControl were hormone deprived and treated for 6 hours with E2 or vehicle. Four biological repliactes were used per condition. Read counts were mapped using Salmon v0.14.1 and Differential expression (DE) was performed using DESeq2 with an FDR (adjusted p-value) < 0.05. Median of ratios normalization was performed across all samples and differentially expressed genes were identified between E2 vs Vehicle and siFEN1 vs siControl conditions. The overlap of these two sets was defined as the FEN1 and E2 responsive genes. Gene Set Enrichment Analysis was performed with clusterProfiler, using all genes ranked by (log2FoldChange * -log10pval).

Transient transfections of siRNA and plasmids

For knockdown experiments 25 nM of single or pooled duplexes of siRNA against FEN1 (Dharmacon MU-010344-01) or a non-targeting control pool (Dharmacon, D-001206-14-20) were transfected with Dharmafect according to manufactures protocol. The expression plasmids pShuttle-FEN1hWT (wild type FEN1) and pShuttle-FEN1DA (D181A point mutant) were kindly provided by Sheila Stewart (Addgene plasmid #35027 and #35028) (12) and cells were transfected with Polyethylenimine (PEI). When appropriate cells were hormone-deprived for 24 hours prior to siRNA transfection or overexpression and further hormone-deprived for 48-72 hours.

Chromatin Immunoprecipitation (ChIP) and Formaldehyde-assisted isolation of regulatory elements (FAIRE)

ChIP experiments were performed as described previously (4) with the following modifications. Three to ten micrograms of antibody was prebound overnight to protein A Dynabeads magnetic beads (Invitrogen). The magnetic bead-chromatin complexes were harvested and washed 10 times with RIPA buffer (50 mM HEPES [pH 7.6], 1 mM EDTA, 0.7% Na deoxycholate, 1% NP-40, 0.5 M LiCl). Antibodies used were anti-ERα (sc-543), anti-FOXA1 (sc-6554), anti-BRG1 (sc-10768), anti-PARP1 (sc-1561) from Santa Cruz Biotechnologies and anti-RNA polymerase II (ab5408), anti-XRCC1 (ab9147) from Abcam. In figure 4, publically available ChIP-seq data was used; ERα (13) and γH2AX (GSE57426) (6). Formaldehyde-assisted isolation of regulatory elements (FAIRE) was performed as described previously (14). ChIP-seq and FAIRE-seq data can be found on GEO: GSE95302

Solexa ChIP and FAIRE sequencing and enrichment analysis

ChIP DNA was amplified as described (15). Sequences were generated by the Illumina Hiseq 2000 genome analyser (using 51 or 65 bp reads), and aligned to the Human Reference Genome (assembly hg19, February 2009). Peak calling over input was performed using MACS peak caller (16) version 1.3.7.1 and DFilter (17), only considering peaks shared by both peak callers. For Figure 2B and Figure 4C all ERα binding regions after 45 minutes of estradiol as published before (13) were used. Details on the number of reads obtained and the percentage of reads aligned can be found below. ChIP-seq and FAIRE-seq data can be found on GEO: GSE95302

Sequencing snapshots and Heatmaps

ChIP-seq data snapshots were generated using the Integrative Genome Viewer IGV 2.2 (www.broadinstitute.org/igv/). Heatmaps were generated using Seqminer, with default settings (18).

mRNA-qPCR expression and ChIP-qPCR

For mRNA expression; cells were treated with vehicle or 100 nM of FEN1 inhibitor after which total RNA was collected by phenol-chloroform extraction. cDNA was made with a Superscript III RT kit (Invitrogen) using manufacturer's protocols after which qPCR was performed. TBP and UBC were used as housekeeping genes. For ChIP: DNA-protein interactions were harvested with ChIP and obtained DNA regions were used after immunoprecipitation. qPCR was performed with SYBR Green (Applied Biosystems) on a Roche LightCycler® 480 Real-Time PCR System using standard protocols. A negative region near the cyclin D1 (CCND1) promoter was used as a negative control. When appropriate an additional negative control primer (Neg 2) was taken along. Primers are described below.

Primers cDNA

Homo sapiens trefoil factor 1 **(TFF1):** FWD ATCGACGTCCCTCCAGAAGA, REV TGGGACTAATCACCGTGCTG; X-box binding protein 1 **(XBP1):** FWD GGGAAGGGCATTTGAAGAAC, REV ATGGATTCTGGCGGTATTGA; retinoic acid receptor alpha **(RARA):** FWD GACCAGATCACCCTCCTCAA, REV GTCCGAGAAGGTCATGGTGT; TATA box binding protein **(TBP):** FWD GTTCTGGGAAAATGGTGTGC, REV GCTGGAAAACCCAACTTCTG; ubiquitin C **(UBC):** FWD ATTTGGGTCGCAGTTCTTG, REV TGCCTTGACATTCTCGATGGT.

Primers ChIP

cyclin D1 **(CCND1) (Neg 1):** FWD TGCCACACACCAGTGACTTT, REV ACAGCCAGAAGCTCCAAAAA; Homo sapiens trefoil factor 1 **(TFF1):** FWD TGGTCAAGCTACATGGAAGG, REV CCATGGGAAAGAGGGACTTT; growth regulation by estrogen in breast cancer 1 **(GREB1):** FWD CACTTTGAGCAAAAGCCACA, REV GCTGCGGCAATCAGAAGTAT; X-box binding protein 1 **(XBP1) :** FWD GGTCACAGGCTGCCAAGTAT, REV AGCCCCAGTTATGGCGTAAT; retinoic acid receptor alpha **(RARA):** FWD CTCAGGACAGGGCAAGAGTG, REV AAGCCACTCCAAGGTAGGTG; Negative control 2 (**Neg 2**): FWD TGGCCCTTGATACTGGAGTC, REV GACATCCAAGGCAAGATGGT; PDZ Domain Containing 1 (**PDZK1**): FWD AGGCCCAGCAAAGACAAATG, REV AAACCACAGGCTGAGGACTG.

Co-Immunoprecipitation

Immunoprecipitations were performed as described previously (19). MCF-7 cells were lysed in RIPA whole cell lysate buffer containing protease inhibitors. Lysates were pre-cleared by incubating with pre-clearing beads (Immunocruz, Santacruz) at 4^{o}C for 2 hours. 5µg of ERα antibody (ER HC20) was incubated with agarose beads (Immunocruz, Santacruz) for 2 hours at 4^{o}C. Agarose beads conjugated with ERα antibody were washed three times with ice-cold PBS and re-suspended in PBS and transferred to the pre-cleared lysates for overnight incubation. Following incubation, beads were washed six times in ice-cold PBS and re-suspended in 2X sample buffer (Sigma, 0.125 M Tris-HCL at pH 6.8, 4% SDS, 20% Glycerol, 10% β-mercaptoethanol and 0.004% bromophenol blue) and heated at 95^{o}C for 10 minutes, and then analyzed by western blot. Antibodies used for IP; anti-ERα (sc-543) from Santacruz, and for WB; anti-ERα (6F11) from Leica Biosystems, anti-AIB1 (BD bioscience, cat no; 611105) and anti-Lamin A/C (sc-7292) and anti-FEN1 (sc-28355) from Santacruz.

Western blot

Cells were lysed with 2x laemmli buffer (containing 1:500 Na3VO4, 1:10 NaF, 1:13 β-Glutamate, 1:100 Protease inhibitors, 1:100 Phosphatase inhibitors). Western blot samples contained 10% DTT and 4% bromophenol blue and were incubated for 5 minutes at 95 °C. Samples were run on 10% SDS-Page gel and transferred to nitrocellulose membranes. Used primary antibodies: anti-p300 (sc-585), anti-FOXA1 (sc-6554), anti-ERα (sc-543) and anti-FEN1 (sc-13051) from Santa Cruz Biotechnologies, anti-RNA polymerase II (ab5408) from Abcam and 1:10.000 actin from Millipore (MAB1501R). Used secondary antibodies: 1:10.000 Licor Odyssey IRDue. Membranes were scanned and analysed with Odyssey V3.0.

Patient cohorts

The discovery-cohort has previously been used and described (20). In short; ERα-positive patients that received tamoxifen in the adjuvant setting, but did not receive adjuvant chemotherapy, were selected from The Netherlands Cancer Institute–Antoni van Leeuwenhoek Hospital (NKI–AVL). Distant metastases were regarded as failure to treatment and used as events. RNA was hybridized on 44 K oligomicroarrays, as described previously (21). The median IHC-score and mRNA expression value was chosen as the cutoff-point.

The validation-cohort has been described before (IKA trial, 1982-1994) (22). In short: ERα-positive patients (no adjuvant chemotherapy) were randomized between 1 year tamoxifen versus no adjuvant therapy. After 1 year a second randomization was performed; 2 additional years of tamoxifen or to stop further treatment. Further patient characteristics and clinical outcome of the original study group (1662 patients) have been described before (23). For 739 patients sufficient

tumor material for IHC was available (23). The median IHC-score value was chosen as the cutoff-point.

Immunohistochemistry

Tissue microarrays (TMAs) were constructed using formalin-fixed paraffin embedded (FFPE) tumor blocks. A total of three (0.6 mm) cores per tumor were embedded in the TMA. TMAs were stained for FEN1 and hematoxylin-eosin (HE) with the ULTRA BenchMark IHC/ISH Staining Module of the NKI. Antibody used was anti-FEN1 (sc-13051) from Santa Cruz Biotechnologies. The percentage of FEN1-positive invasive tumor cells were scored. One TMA was scored independently in a blinded manner by a second observer to calculate inter-observer variability (κ=0.708). The inter-observer variability was analyzed using the (weighted) Cohen's kappa coefficient.

For ex-vivo tumor cultures, tissue sections were incubated with a Ki67 primary antibody (MIB1 1:400; DAKO M7240 Glostrup, Denmark) at 4C overnight followed by detection using a biotinylated anti-mouse secondary antibody at 1:400 dilution (DAKO E0433, Glostrup, Denmark) for 30 min followed by incubation with horseradish peroxidase-conjugated streptavidin (DAKO P0397, Glostrup, Denmark). Visualization of immunostaining was performed using 3,3-diaminobenzidine (Sigma D9015).

Statistics

PAM (24) was performed to determine the minimum number of genes required to attain accurate separation of good and poor survival. Here, good and poor survival was defined based on whether or not a distant metastasis occurred within five years. The number of genes was selected

such that the area under the ROC curve (AUC) was optimized in a 10-fold cross validation. Subsequently, Lasso-penalized logistic regression (25) was used to obtain a robust selection of the best performing genes across two cohorts (26,27). To this end, 1,000 cross-validation analyses were performed for each cohort to select gene subsets optimizing the AUC. Genes were then ranked according to how many times they were part of the optimal gene set in either of the two cohorts. Finally, the previously determined optimal number of genes were selected starting from the highest ranked gene.

Pearson's correlation coefficient was used to assess the correlation between relative FEN1 mRNA levels and FEN1 IHC scores. Survival curves were constructed using the Kaplan-Meier method and compared using log-rank test. Unadjusted and adjusted Cox proportional hazard regression analyses were performed; for the discovery-cohort the covariates age (<60 versus ≥60), diameter of the tumor (≤20 mm versus 20-50 mm versus >50 mm), tumor grade (grade 1 versus grade 2 versus grade 3) and the number of affected lymph nodes (Negative versus 1-3 versus ≥4); and for the validation-cohort the covariates age (< 65 versus ≥ 65), grade (grade 1-2 versus grade 3), tumor stage (T1-T2 versus T3-4), HER2 status (negative versus positive), PgR status (negative versus positive). In the validation-cohort all analyses were stratified for nodal status (negative versus positive) because lymph node positive patients, after 1989, skipped the first randomization and all received 1 year of tamoxifen. A p-value <0.05 was considered as a significant result and FEN1 levels were used a binary factor to assess the interaction with adjuvant treatment. A two-tailed Student's t-test was performed when appropriate.

Immunofluorescence

Immunofluorescence analysis was performed as described previously (6). Briefly, hormone-deprived MCF-7 cells were cultured on glass coverslips before the addition of 10 nM E2. Additionally cells were pretreated with 100 nM of FEN1 inhibitor as appropriate. Cells were fixed with 4% paraformaldehyde for 10 minutes and permeabilized with 0.2% Triton X-100. Used primary antibody was γH2AX (05-636, Millipore) and for secondary Alexa fluor 488 (Invitrogen) was used. ToPro (Invitrogen) nuclear dye was used to visualize nuclei. Images were acquired using a Carl Zeiss confocal microscope using LSM 510 image browser. Images were analyzed using Fuji Image J (NIH, USA) and Cell Profiler (Broad Institute, USA) to quantify number of foci per cell.

Primary ex-vivo tumor cultures

Breast tumor samples and relevant clinical data were obtained from women undergoing surgery at the Burnside Private Hospital, Adelaide, South Australia, with written informed consent. This study was approved by the University of Adelaide Human Research Ethics Committee (approval numbers: H-065-2005; H-169-2011). Following surgery, excised tissue samples were cultured ex vivo as described previously previously (28,29). Briefly, tumor pieces were cultured on gelatin sponges in full medium containing a vehicle, FEN1 inhibitor (200 nM) or, when enough material was present, tamoxifen (2 uM). After 3 to 6 days, tissue was fixed in 4% formalin in phosphate-buffered saline (PBS) at 4 °C overnight and subsequently processed into paraffin blocks. Slices (2 μm) were stained with haematoxylin and eosin or Ki67 and examined by a pathologist to confirm the presence/proportion of tumor cells. Tumor slides were scored by a pathologist for the percentage of Ki67 positive tumor cells.

FEN1 inhibitor screen

The previously reported non-radioactive FEN1 activity assay (30) was combined with a quantitative high throughput screen (qHTS) (31) and implemented on a fully integrated robotic system (32), utilizing a large scale chemical library arrayed in qHTS-formatted 1536-well based plates (33). A total of 465,195 compounds were tested. Automated large-scale curve fitting and classification of curve types were determined (31). Using this classification, 3,543 compounds were considered inconclusive or weak inhibitors due to either lower quality curves or moderate inhibition. Another 1,123 compounds demonstrated a dose dependent increase of fluorescent signal, but were regarded as likely inactive due to suspected auto-fluorescence, which was observed in the initial background read. A total of 2,485 compounds were categorized as active FEN1 inhibitors and as part of the NIH Molecular Libraries Program (https://commonfund.nih.gov/molecularlibraries) profiled for their effect in over 150 biochemical and cell-based assays. Furthermore, cheminformatics filters were applied to the chemical library to annotate compounds for their reactivity (34). See also PubChem AID: 488816, 588795 and 720498.

Results

FEN1 levels correlate with breast cancer patient survival after tamoxifen treatment

In a previous report, we identified 111 genes that predict outcome in tamoxifen-treated ERα-positive breast cancer patients (4). To reveal drivers causally involved in the observed patient outcome, we refined the gene signature to identify a minimal set of genes without losing predictive capacity (Figure 1A). Computationally minimizing the 111-gene classifier by Prediction Analysis for Microarrays (PAM) (24) and Lasso-penalized logistic regression (25) in

two independent cohorts of tamoxifen-treated patients (26,27) illustrated that the classifier could be reduced to four genes before losing its stratification potential: FEN1, MCM2, STARD13 and HBP1 (Figure 1A). Validation of the four genes in the METABRIC dataset (35) demonstrated that only FEN1 was significant by multivariate analysis in ERα-positive, but not ERα-negative cases (Sup Fig S1A), suggesting FEN1 is selectively associated with outcome in ERα-positive breast cancer.

To assess the clinical impact of both FEN1 mRNA and protein levels as a single-gene classifier on survival, we first used samples of ERα-positive cases that received adjuvant tamoxifen (Discovery-cohort) (20), using microarray-based ("mRNA") and immunohistochemistry-based ("IHC") FEN1 expression ranging from 0-100% positive tumor cells (Figure 1B), which correlated with FEN1 mRNA levels (Pearson correlation coefficient=0.58) (Figure 1C). For both mRNA and IHC, the median was used to stratify patients into "Low" and "High" FEN1 groups (Figure 1D). FEN1 mRNA (HR: 2.46, p=0.006) (Figure 1E) (Sup table S1) and protein (HR: 2.05, p=0.041) (Figure 1F) (Sup table S1) expression were associated with Distant Metastasis-Free Survival (DMFS), with high FEN1 levels correlating with a poor survival.

To validate these findings in an independent cohort and to further investigate whether FEN1 associates with disease progression (prognostic classifier) or whether its levels are informative for treatment response (predictive classifier), we utilized tissue from a cohort where patients were randomized between tamoxifen or no adjuvant endocrine therapy (Validation cohort) (22). As this cohort contains a matched non-tamoxifen treated group, it can provide an extra level of evidence with regards to predictive potential which is not available from other tamoxifen cohorts that lack a non-endocrine treated control group (36).

In this validation cohort, FEN1 was associated with Recurrence-Free Survival (RFS) in ERα-positive patients (n=389) (HR=1.90, p=0.002) (Figure 1G), also after multivariate correction for age, tumor grade, tumor stage, HER2, PgR and lymph node status (adjusted HR=1.58, p=0.047) (Sup Table S1), which was successfully confirmed in the METABRIC dataset (Sup Fig S1A,B). No association was found between FEN1 levels and RFS in ERα-negative breast cancer patients (n=127) (HR=1.29, p=0.35) (Figure 1G and Sup Fig S1B). To make sure this difference in significant association with RFS was not due to the difference in patient numbers, we down sampled the ERα-positive patients group to n=127 (matching the ERα-negative group) showing that FEN1 levels were still significantly associated with RFS (Log Rank p=0.028; Cox regression HR=2.19, p=0.033) (Sup Fig S1C). Furthermore, high FEN1 significantly correlated with poor outcome in tamoxifen-treated patients (HR=2.05, p=0.003), but not for patients not receiving endocrine therapy (HR=1.37, p=0.436) (Figure 1H) (Sup table S1).

Next, we stratified patients according to FEN1 levels and categorized by tamoxifen treatment (Figure 1I). Patients with high FEN1 did not benefit from tamoxifen (HR=0.67, p=0.217), while tamoxifen-treated patients with low FEN1 had a better survival as compared to those who did not receive adjuvant tamoxifen (HR=0.35, p=0.007), also after multivariate correction (high FEN1 adjusted HR=0.67, p=0.213; low FEN1 adjusted HR=0.39, p=0.015) (Sup table S1). The predictive potential of FEN1 levels was further illustrated by the interaction test between FEN1 levels and hormonal therapy status (HR=2.19, p<0.001; adjusted HR=1.86, p<0.001)

As the standard regimens of hormonal treatment for ERα-positive breast cancer have changed since the time of our validation cohort (e.g. 3 years of tamoxifen then versus 2-3 years

of tamoxifen followed by 5 years of an aromatase inhibitor now), we tested how FEN1 levels would perform in a cohort using more contemporary hormonal therapies (METABRIC). In patients treated with hormonal therapy, high FEN1 was associated poor disease-specific survival (HR=2.09, p<0.001), also after multivariate correction (adjusted HR=1.83, p<0.001) (Sup Figure S1D). Additionally, we assessed whether the menopausal status of a patient would influence the performance of FEN1 as predictive biomarker, as in the clinical setting tamoxifen is predominately used in pre-menopausal women. Both in premenopausal (HR=5.29, p<0.001) and postmenopausal patients (HR=1.79, p<0.001), FEN1 levels were significantly associated with patient outcome, also after multivariate correction (premenopausal adjusted HR=5.57, p<0.001; postmenopausal adjusted HR=1.62, p<0.001) (Sup Figure S1E). Although significant in both menopausal states, the predictive potential of FEN1 appeared stronger in the premenopausal setting (HR5.57 vs HR=1.62).

In summary, FEN1 levels are not indicative of outcome in ERα-negative breast cancers, nor in ERα-positive disease in the absence of adjuvant endocrine therapy. Only in ERα-positive patients who were treated with tamoxifen, FEN1 levels were associated with poor outcome, rendering FEN1 a predictive marker for tamoxifen treatment response.

FEN1 is essential for ERα-chromatin interactions and transcriptional complex formation

FEN1 functions as a predictive marker for tamoxifen resistance in ERα–positive breast cancer. To determine whether FEN1 directly affects ERα activity, we tested if FEN1 is recruited to the ERα genomic complex. Based on co-immunoprecipitations in MCF-7 cells, endogenous ERα and FEN1 interact in an estradiol-dependent fashion, which is comparable to the recruitment of SRC3 and p300 to the ERα complex (Figure 2A). Strikingly, recruitment of SRC3 and p300 was greatly reduced upon FEN1 knockdown, implying a direct role for FEN1 in the

formation of the ERα transcriptional complex (Figure 2A). Additionally, knockdown of FEN1 (Sup Fig S2A; knockdown validation) abrogated ERα-chromatin interactions (Figure 2B,C and Sup Table S2), which coincided with a loss of RNA Polymerase II at these sites (Sup Fig S2B). Of note, both motif enrichment (Figure 2D) and genomic distribution (Figure 2E) of siFEN1 affected ERα-chromatin interactions, demonstrate that siFEN1 results in the loss of 'regular canonical ERα sites', and is unselective for specific motifs or genomic elements. In contrast to ERα, FOXA1 chromatin binding (Figure 2B,C and Sup Fig S2B) and chromatin accessibility (Figure 2F) was not decreased by siFEN1, implicating FEN1 as a regulator of ERα-chromatin interactions downstream of FOXA1.

FEN1 impacts ERα-mediated transcription and cell proliferation

The above results demonstrate that FEN1 modulates ERα-chromatin interactions and transcription complex formation. Next, we assessed what the effect of FEN1 is on ERα-mediated transcription. RNA-seq demonstrated that upon E2 treatment 1298 genes were differentially expressed in siControl cells (Figure 3A) while knockdown of FEN1 levels resulted in 218 differential expressed genes (Figure 3B). In this list of FEN1 responsive genes a significant enrichment for E2-responsive genes was found (Fisher's exact test; p-value=3.9e-25), with around 24% (54 genes) overlapping with E2 responsive genes (Figure 3C). Gene set enrichment analysis of the E2 and FEN1 responsive genes showed a significant enrichment for the Hallmark Estrogen Response Late genes (Figure 3D; full list Sup Fig S3A).

As the Hallmark Estrogen Response Late genes were enriched in FEN1 and E2 repsonsive genes, we next assesed what the effect of this would be on ERα-mediated proliferation. FEN1 knockdown in MCF-7 cells decreased ERα-mediated cell growth under

DMSO and E2 conditions (Figure 3E; siRNA deconvolution in Sup Fig S3B), while FEN1 overexpression increased cell proliferation under these conditions (Figure 3F). The observed decrease in cell proliferation after siFEN1 was validated in ERα-positive T47D cells (Sup Fig S3C). Both in tamoxifen and fulvestrant (a selective estrogen receptor down-regulator) treated cells, FEN1 knockdown didn't result in substantial growth deffects (Fig 3E,F). Moreover, neither FEN1 knockdown in ERα-negative MDA-MB-231 or CAL120 cells (Figure 3G), affected cell proliferation, implicating that the observed effects are mediated through ERα and not broadly related to the role of FEN1 in DNA replication (37). Cumulatively, we demonstrate that FEN1 impacts ERα-mediated transcription and cell proliferation.

FEN1 inhibition perturbs ERα-activation and stability

Given FEN1's key role in modulating ERα-activity, we hypothesized a FEN1 inhibitor could have great therapeutic potential in treating ERα-positive breast cancer. Since FEN1 inhibitors have been developed before on a small scale (38,39) but were not effective in breast cancer cell lines as single agent (40), other more-potent inhibitors could still be found. Therefore, we performed a small-molecule compound screen of 465,195 compounds, tested at six different concentrations, to identify novel inhibitors of FEN1's flap-cleaving activity. A previously reported non-radioactive FEN1 activity assay was used (30) in which a small DNA product containing fluorophore donor 6-TAMRA (6-Carboxytetramethylrhodamine) is cleaved and released by FEN1 from a DNA flap structure labeled with a fluorescent quencher (Black Hole Quencher 2), resulting in measurable fluorescence (Figure 4A). A quantitative high throughput robotics screen (31) was performed on 465,195 compounds (33), identifying 2,485 active FEN1 inhibitors (Figure 4B and Sup Fig S4A). As part of the NIH Molecular Libraries Program

(https://commonfund.nih.gov/molecularlibraries), these compounds have been profiled for their effect in >150 biochemical and cell-based assays including DNA-repair and related screens (e.g. APE1, POLB, POLK, POLH, POLI, PCNA, DNA binding) (Sup Fig S4B and Sup Table S3). Furthermore, cheminformatics filters have been applied to annotate compounds for their reactivity (34). The selectivity profiling data and filters for reactive functional groups were used to triage the 2,485 active FEN1 inhibitors, and a set of 22 inhibitors was selected for further biological validation.

After testing the 22 hits on MCF-7 cell proliferation, we continued with the three most-potent hits for further validation (Sup Fig S4C) and selected FENi#2 (MLS002701801) as most potent and promising hit (Figure 4B and Sup Fig S4B,C) (Sup Table S3).

Previously it was shown that ERα-cofactor APOBEC3B can induce C-to-U modifications and UNG recruitment at ERα binding sites, resulting in the induction of abasic regions of DNA which regulate ERα-mediated transcriptional activity (6). As abasic DNA can be repaired through the Base Excision Repair (BER) pathway (7), we hypothesized FEN1 might be functionally involved in a long-patch BER response following the formation of abasic sites, thereby regulating ERα-activity. In agreement with a BER response near ERα-binding sites, we observed BER-members XRCC1 and PARP1 (7), to bind these genomic regions (Figure 4C and Sup Fig S4D), with PARP1 being previously described as co-regulator of ERα (41). The APOBEC3B induced C-to-U modifications were shown to ultimately give rise to γH2AX formation at ERα sites (6), as assessed by ChIP-seq (Figure 4D and Sup Fig S4E,F). This γH2AX-induction was validated by immunofluorescence, where 15 minutes of E2 stimulation induced γH2AX foci (Figure 4E,F). FEN1 inhibition through 100 nM FENi#2 blocked this E2-induced γH2AX-formation (Figure 4E,F and Sup Fig S4G) and could not be explained by lower

ERα-chromatin interactions at time points preceding DNA damage (10 minutes after E2 stimulation) (Figure 4G and Sup Fig S4H). Interestingly, when assessing ERα and PARP1 binding after 30 minutes of E2 stimulation, which is after the yH2AX induction found at 10', FEN1 inhibition did decrease ERα and PARP1 chromatin binding (Figure 4G and Sup Fig S4H), which suggests that FEN1 perturbation effects on ERα binding only occur after the moment of γH2AX-formation (10 min after E2 induction). In line with the known role of γH2AX in promoting chromatin remodeling (42), FEN1 inhibition decreased both γH2AX formation and recruitment of BRG1; the catalytic subunit of the SWI/SNF chromatin remodeling complex (42) (Figure 4G and Sup Fig S4H), which chromatin interactions overlapped ERα binding sites. Altogether this indicates that FEN1 plays a functional role during the induction of yH2AX and subsequent ERα and coregulator binding capacity.

An additional aspect of FEN1's regulatory role in ERα-activity was found in the E2-induced proteasomal degradation of ERα (43). Herein FEN1 inhibition enhanced E2-induced ERα-degradation (Sup Fig S4I) while pretreatment with proteasome inhibitor MG132 prevented this FENi#2-induced reduction of ERα-chromatin interactions (Sup Fig S4I). This together with the observation that ERα-chromatin interactions were not affected by FEN1 inhibition until the moment of yH2AX induction (Figure 4G and Sup Fig S4H), favors a model wherein FEN1 regulates ERα-chromatin binding by preventing E2-induced proteasomal degradation.

Cumulatively, we identify FENi#2 as a potent and specific FEN1 inhibitor, and demonstrate that FEN1 regulates ERα-activity through the functional formation of yH2AX –and subsequent BRG1 recruitment- and can regulate ERα-chromatin interactions by inhibiting proteasome-mediated degradation. Additionally, we provide evidence that additional BER-members (PARP1 and XRCC1) are also present at sites of ERα binding.

FEN1 inhibition as novel drug option in tamoxifen resistant breast cancer

Since tamoxifen-resistant cell lines (13) and tumors (44) still require ERα function, an alternative mode of blocking ERα action through FEN1 inhibition would have strong clinical potential.

To assess this, we investigated the effect of FENi#2 on ERα binding and induced gene expression. First, the optimal time point of ERα-chromatin interactions after E2 treatment was determined, with 30 minutes of E2 stimulation resulting in maximum detection of ERα-chromatin interactions (Figure 5A). Overnight pretreatment with 100 nM FENi#2 significantly inhibited these E2-induced ERα-chromatin interactions and ERα-driven gene transcription (Figure 5B), analogous to siFEN1 (Figure 2). This inhibition of ERα-activity by FENi#2 showed a notable overlap with siFEN1, both in reduced cell growth as in ERα-binding perturbation (Sup Fig S5A,B). In the absence of E2, ERα protein levels were unaffected by FENi#2 (Sup Fig S5C), indicating decreased ERα-chromatin interactions and gene transcription were not due to reduced initial amounts of ERα protein.

Colony formation assays were performed for a panel of human breast cancer cell lines; (a) MCF-7 and T47D (ERα+), (b) MCF7-T and TAMR (tamoxifen resistant MCF-7 derivatives (45,46)) and (c) BT-20 and CAL-120 (ERα-). Cells were treated with increasing concentrations of FENi#2 in the presence or absence of tamoxifen (Figure 5C,D), confirming tamoxifen responsiveness of the sensitive cell lines (Figure 5C,D). Proliferation of MCF-7 and T47D cells was inhibited in a dose-dependent manner with IC_{50} values of 69 and 78 nM of the inhibitor, respectively (Sup table S4). In contrast, sensitivity to FENi#2 for ERα-negative cell lines BT-20 and CAL120 was limited, with an IC_{50} of 314 nM in BT20, while not reaching 50% inhibition in

CAL120 cells. Interestingly, tamoxifen resistant MCF-7 derivatives showed enhanced sensitivity to FEN1 inhibition in relation to the parental cells (IC_{50}= 29 nM for both tamoxifen resistant cell lines).

To validate the efficacy of FEN1 inhibition in ERα-positive breast cancer, we used *ex vivo* primary ERα-positive tumor cultures (i.e. explants) (28,29) in the presence or absence of compound FENi#2. Tumors were cut into small pieces and randomized between vehicle, FEN1 inhibitor or tamoxifen treatments and cultured for 3-6 days on gelatin sponges, allowing sustained tissue architecture and viability (29). Explants were stained for cell proliferation marker Ki67 and scored by a pathologist. Upon FEN1 inhibition, all four tumor explants demonstrated reduced proliferation (Ki67) (Figure 5E,F). For 3 out of 4 explants, sufficient material was available for a tamoxifen group, demonstrating comparable reductions in Ki67 signal (Sup Fig S5D).

Taken together, we show that pharmacological inhibition of FEN1 efficiently blocks ERα-driven tumor cell proliferation, with enhanced potency in tamoxifen-resistant cells. As FEN1 perturbation inhibits primary tumor tissue growth, we demonstrate therapeutic potential of our FEN1 inhibitor in the treatment of ERα-positive cancer.

Discussion

Several multi-gene prognostic classifiers have been reported that stratify breast cancer patients on outcome (47). Most of these classifiers lack biological insights regarding the drivers of tumor progression. Here, we refined a 111-gene classifier to a single gene predictor of disease outcome, revealing a drug target with clinical potential in the treatment of tamoxifen resistant breast tumors. We identified FEN1 as a predictive marker for tamoxifen resistance in clinical

specimens, with potential for outcome-prediction exclusive in ERα-positive breast cancers. Before any clinical implication of FEN1 as a predictive marker however, the predictive versus prognostic potential of FEN1 needs to be validated in an independent second randomized clinical trial of tamoxifen versus placebo. Of note, previous work from Abdel-Fatah et al. describes FEN1 protein levels to correlate with a poor outcome in ERα-positive as well as in ERα-negative breast cancer patients (11). This discrepancy might be best explained by the use of different antibodies used for IHC and the fact that Abdel-Fatah et al. also reported cytoplasmic staining (11), which was absent in our stainings. Our observation that FEN1 has predictive potential in ERα-positive cases is in line with our cell proliferation analyses, where perturbation of FEN1 was only effective in ERα-positive cell lines, while yielding no detectable effects in ERα-negative cells.

Accumulating evidence repositions DNA repair factors as coactivators of transcription, amongst other in facilitating chromatin remodeling (5). Chromatin remodeling at ERα-binding regions can be initiated by BRG1 (48), the recruitment of which is promoted by γH2AX (42). Failure to induce γH2AX-signaling at ERα regions diminished BRG1 recruitment (6), implicating ERα-induced γH2AX as facilitator of chromatin remodeling. We found FEN1 to be critically involved in this process and can thereby regulate BRG1 recruitment, and ultimately enable transcription. Interestingly enough, we observed that the decrease in ERα chromatin binding by FEN1 inhibition only seem to occur after the moment of γH2AX-formation (Fig 4G). Besides BRG1, we demonstrate that SRC3 and p300 recruitment to ERα-transcriptional complex is also dependent on FEN1. Additionally, FEN1 inhibition enhanced E2-induced ERα-degradation, mediated by proteasomal activity (43). Consequently, this favors a model wherein, along with being crucial for cofactor recruitment (as exemplified by SRC3, p300 and BRG1),

FEN1 can also alter ERα's activity by regulating the stability of its chromatin binding after activation by E2.

Transcription-coupled degradation of the ERα is well known for many years (43,49-51) , but still not fully understood. Interestingly, inhibiting FEN1 resulted in a ligand-driven loss of ERα chromatin interactions, which associates with a loss of ERα protein levels, suggesting that FEN1 inhibition could potentially uncouple transcriptional events from proteasome-mediated degradation of the receptor. Further studies should be aimed to further elucidate this mechanism, and determine how FEN1 is mechanistically involved in this.

Small molecule–mediated inhibition of FEN1 functionally abrogated ERα-activity and ultimately blocked human tumor explant proliferation. With an inhibitor effective in the nM-range, we illustrate that FEN1 inhibition might yield a promising novel therapy for ERα-positive breast cancer. While FEN1 inhibition has been described before, it has mainly been linked to chemosensitization (52,53) or as a part of synthetic lethal interactions (38,54), but not as an effective therapeutic strategy on its own (40). Although it is widely accepted that most small molecule inhibitors aren't truly specific for their targets, including most clinically-applied small molecules (55), our FEN1 inhibitor was inactive in almost all of the 150 additional protein assays we investigated (Sup Fig S4B and Sub Table S3). Even though the effect of siFEN1 and the inhibitor were very similar, there could still be some off-target effects making additional chemical matter refinements required for further clinical development of FEN1 targeting in breast cancer. Here we report the first effective single-agent application of FEN1 inhibition by specifically targeting ERα-positive breast cancer. Most importantly, tamoxifen resistant cell lines showed an increased sensitivity for FEN1 blockade; a feature that could possibly be exploited in

the treatment of advanced breast cancer, thereby providing a novel targeted therapy in case of tamoxifen resistance.

Acknowledgments

The authors thank Ron Kerkhoven from the NKI Genomics Core Facility. The authors thank Sheila Stewart (Department of Cell Biology and Physiology, Washington University in St. Louis, USA) for providing pShuttle-FEN1hWT and pShuttle-D181A, Robert Nicholson (Cardiff School of Pharmacy and Pharmaceutical Science, Cardiff University, UK) for providing the TAM-R cells, Kenneth Nephew (Indiana University, School of Medicine, USA) for providing MCF7-T cells. The authors thank Hongmao Sun and David Maloney (National Center for Advancing Translational Sciences, National Institutes of Health, USA) for the additional design and analyses of the FEN1 HTS inhibitor screen and synthesis of required protein and reagents.

References

1. Glass, C.K., Rose, D.W. and Rosenfeld, M.G. (1997) Nuclear receptor coactivators. *Curr Opin Cell Biol*, **9**, 222-232.
2. Jordan, V.C. and Murphy, C.S. (1990) Endocrine pharmacology of antiestrogens as antitumor agents. *Endocrine reviews*, **11**, 578-610.
3. Shou, J., Massarweh, S., Osborne, C.K., Wakeling, A.E., Ali, S., Weiss, H. and Schiff, R. (2004) Mechanisms of tamoxifen resistance: increased estrogen receptor-HER2/neu cross-talk in ER/HER2-positive breast cancer. *Journal of the National Cancer Institute*, **96**, 926-935.
4. Zwart, W., Theodorou, V., Kok, M., Canisius, S., Linn, S. and Carroll, J.S. (2011) Oestrogen receptor-co-factor-chromatin specificity in the transcriptional regulation of breast cancer. *The EMBO journal*, **30**, 4764-4776.
5. Fong, Y.W., Cattoglio, C. and Tjian, R. (2013) The intertwined roles of transcription and repair proteins. *Molecular cell*, **52**, 291-302.
6. Periyasamy, M., Patel, H., Lai, C.F., Nguyen, V.T., Nevedomskaya, E., Harrod, A., Russell, R., Remenyi, J., Ochocka, A.M., Thomas, R.S. *et al.* (2015) APOBEC3B-Mediated Cytidine Deamination Is Required for Estrogen Receptor Action in Breast Cancer. *Cell reports*, **13**, 108-121.

7. Krokan, H.E. and Bjoras, M. (2013) Base excision repair. *Cold Spring Harbor perspectives in biology*, **5**, a012583.
8. Zheng, L. and Shen, B. (2011) Okazaki fragment maturation: nucleases take centre stage. *Journal of molecular cell biology*, **3**, 23-30.
9. Singh, P., Yang, M., Dai, H., Yu, D., Huang, Q., Tan, W., Kernstine, K.H., Lin, D. and Shen, B. (2008) Overexpression and hypomethylation of flap endonuclease 1 gene in breast and other cancers. *Molecular cancer research : MCR*, **6**, 1710-1717.
10. Schultz-Norton, J.R., Walt, K.A., Ziegler, Y.S., McLeod, I.X., Yates, J.R., Raetzman, L.T. and Nardulli, A.M. (2007) The deoxyribonucleic acid repair protein flap endonuclease-1 modulates estrogen-responsive gene expression. *Molecular endocrinology*, **21**, 1569-1580.
11. Abdel-Fatah, T.M., Russell, R., Albarakati, N., Maloney, D.J., Dorjsuren, D., Rueda, O.M., Moseley, P., Mohan, V., Sun, H., Abbotts, R. *et al.* (2014) Genomic and protein expression analysis reveals flap endonuclease 1 (FEN1) as a key biomarker in breast and ovarian cancer. *Mol Oncol*.
12. Saharia, A., Teasley, D.C., Duxin, J.P., Dao, B., Chiappinelli, K.B. and Stewart, S.A. (2010) FEN1 ensures telomere stability by facilitating replication fork re-initiation. *The Journal of biological chemistry*, **285**, 27057-27066.
13. Hurtado, A., Holmes, K.A., Ross-Innes, C.S., Schmidt, D. and Carroll, J.S. (2011) FOXA1 is a key determinant of estrogen receptor function and endocrine response. *Nature genetics*, **43**, 27-33.
14. Giresi, P.G. and Lieb, J.D. (2009) Isolation of active regulatory elements from eukaryotic chromatin using FAIRE (Formaldehyde Assisted Isolation of Regulatory Elements). *Methods*, **48**, 233-239.
15. Jansen, M.P., Knijnenburg, T., Reijm, E.A., Simon, I., Kerkhoven, R., Droog, M., Velds, A., van Laere, S., Dirix, L., Alexi, X. *et al.* (2013) Hallmarks of aromatase inhibitor drug resistance revealed by epigenetic profiling in breast cancer. *Cancer Res*, **73**, 6632-6641.
16. Zhang, Y., Liu, T., Meyer, C.A., Eeckhoute, J., Johnson, D.S., Bernstein, B.E., Nusbaum, C., Myers, R.M., Brown, M., Li, W. *et al.* (2008) Model-based analysis of ChIP-Seq (MACS). *Genome biology*, **9**, R137.
17. Kumar, V., Muratani, M., Rayan, N.A., Kraus, P., Lufkin, T., Ng, H.H. and Prabhakar, S. (2013) Uniform, optimal signal processing of mapped deep-sequencing data. *Nature biotechnology*, **31**, 615-622.
18. Ye, T., Krebs, A.R., Choukrallah, M.A., Keime, C., Plewniak, F., Davidson, I. and Tora, L. (2011) seqMINER: an integrated ChIP-seq data interpretation platform. *Nucleic acids research*, **39**, e35.
19. Lopez-Garcia, J., Periyasamy, M., Thomas, R.S., Christian, M., Leao, M., Jat, P., Kindle, K.B., Heery, D.M., Parker, M.G., Buluwela, L. *et al.* (2006) ZNF366 is an estrogen receptor corepressor that acts through CtBP and histone deacetylases. *Nucleic acids research*, **34**, 6126-6136.
20. Kok, M., Holm-Wigerup, C., Hauptmann, M., Michalides, R., Stal, O., Linn, S. and Landberg, G. (2009) Estrogen receptor-alpha phosphorylation at serine-118 and tamoxifen response in breast cancer. *Journal of the National Cancer Institute*, **101**, 1725-1729.
21. Kok, M., Linn, S.C., Van Laar, R.K., Jansen, M.P., van den Berg, T.M., Delahaye, L.J., Glas, A.M., Peterse, J.L., Hauptmann, M., Foekens, J.A. *et al.* (2009) Comparison of

gene expression profiles predicting progression in breast cancer patients treated with tamoxifen. *Breast cancer research and treatment*, **113**, 275-283.
22. Michalides, R., van Tinteren, H., Balkenende, A., Vermorken, J.B., Benraadt, J., Huldij, J. and van Diest, P. (2002) Cyclin A is a prognostic indicator in early stage breast cancer with and without tamoxifen treatment. *Br J Cancer*, **86**, 402-408.
23. Beelen, K., Opdam, M., Severson, T.M., Koornstra, R.H., Vincent, A.D., Wesseling, J., Muris, J.J., Berns, E.M., Vermorken, J.B., van Diest, P.J. *et al.* (2014) Phosphorylated p-70S6K predicts tamoxifen resistance in postmenopausal breast cancer patients randomized between adjuvant tamoxifen versus no systemic treatment. *Breast cancer research : BCR*, **16**, R6.
24. Tibshirani, R., Hastie, T., Narasimhan, B. and Chu, G. (2002) Diagnosis of multiple cancer types by shrunken centroids of gene expression. *Proc Natl Acad Sci U S A*, **99**, 6567-6572.
25. Friedman, J., Hastie, T. and Tibshirani, R. (2010) Regularization Paths for Generalized Linear Models via Coordinate Descent. *Journal of statistical software*, **33**, 1-22.
26. Loi, S., Haibe-Kains, B., Desmedt, C., Lallemand, F., Tutt, A.M., Gillet, C., Ellis, P., Harris, A., Bergh, J., Foekens, J.A. *et al.* (2007) Definition of clinically distinct molecular subtypes in estrogen receptor-positive breast carcinomas through genomic grade. *J Clin Oncol*, **25**, 1239-1246.
27. Buffa, F.M., Camps, C., Winchester, L., Snell, C.E., Gee, H.E., Sheldon, H., Taylor, M., Harris, A.L. and Ragoussis, J. (2011) microRNA-associated progression pathways and potential therapeutic targets identified by integrated mRNA and microRNA expression profiling in breast cancer. *Cancer Res*, **71**, 5635-5645.
28. Dean, J.L., McClendon, A.K., Hickey, T.E., Butler, L.M., Tilley, W.D., Witkiewicz, A.K. and Knudsen, E.S. (2012) Therapeutic response to CDK4/6 inhibition in breast cancer defined by ex vivo analyses of human tumors. *Cell cycle*, **11**, 2756-2761.
29. Mohammed, H., Russell, I.A., Stark, R., Rueda, O.M., Hickey, T.E., Tarulli, G.A., Serandour, A.A., Birrell, S.N., Bruna, A., Saadi, A. *et al.* (2015) Progesterone receptor modulates ERalpha action in breast cancer. *Nature*, **523**, 313-317.
30. Dorjsuren, D., Kim, D., Maloney, D.J., Wilson, D.M., 3rd and Simeonov, A. (2011) Complementary non-radioactive assays for investigation of human flap endonuclease 1 activity. *Nucleic acids research*, **39**, e11.
31. Inglese, J., Auld, D.S., Jadhav, A., Johnson, R.L., Simeonov, A., Yasgar, A., Zheng, W. and Austin, C.P. (2006) Quantitative high-throughput screening: a titration-based approach that efficiently identifies biological activities in large chemical libraries. *Proc Natl Acad Sci U S A*, **103**, 11473-11478.
32. Michael, S., Auld, D., Klumpp, C., Jadhav, A., Zheng, W., Thorne, N., Austin, C.P., Inglese, J. and Simeonov, A. (2008) A robotic platform for quantitative high-throughput screening. *Assay and drug development technologies*, **6**, 637-657.
33. Yasgar, A., Shinn, P., Jadhav, A., Auld, D., Michael, S., Zheng, W., Austin, C.P., Inglese, J. and Simeonov, A. (2008) Compound Management for Quantitative High-Throughput Screening. *Jala*, **13**, 79-89.
34. Jadhav, A., Ferreira, R.S., Klumpp, C., Mott, B.T., Austin, C.P., Inglese, J., Thomas, C.J., Maloney, D.J., Shoichet, B.K. and Simeonov, A. (2010) Quantitative analyses of aggregation, autofluorescence, and reactivity artifacts in a screen for inhibitors of a thiol protease. *Journal of medicinal chemistry*, **53**, 37-51.

35. Curtis, C., Shah, S.P., Chin, S.F., Turashvili, G., Rueda, O.M., Dunning, M.J., Speed, D., Lynch, A.G., Samarajiwa, S., Yuan, Y. *et al.* (2012) The genomic and transcriptomic architecture of 2,000 breast tumours reveals novel subgroups. *Nature*, **486**, 346-352.
36. Beelen, K., Zwart, W. and Linn, S.C. (2012) Can predictive biomarkers in breast cancer guide adjuvant endocrine therapy? *Nat Rev Clin Oncol*, **9**, 529-541.
37. Zheng, L., Jia, J., Finger, L.D., Guo, Z., Zer, C. and Shen, B. (2011) Functional regulation of FEN1 nuclease and its link to cancer. *Nucleic acids research*, **39**, 781-794.
38. van Pel, D.M., Barrett, I.J., Shimizu, Y., Sajesh, B.V., Guppy, B.J., Pfeifer, T., McManus, K.J. and Hieter, P. (2013) An evolutionarily conserved synthetic lethal interaction network identifies FEN1 as a broad-spectrum target for anticancer therapeutic development. *PLoS genetics*, **9**, e1003254.
39. Tumey, L.N., Bom, D., Huck, B., Gleason, E., Wang, J., Silver, D., Brunden, K., Boozer, S., Rundlett, S., Sherf, B. *et al.* (2005) The identification and optimization of a N-hydroxy urea series of flap endonuclease 1 inhibitors. *Bioorg Med Chem Lett*, **15**, 277-281.
40. Exell, J.C., Thompson, M.J., Finger, L.D., Shaw, S.J., Debreczeni, J., Ward, T.A., McWhirter, C., Sioberg, C.L., Martinez Molina, D., Abbott, W.M. *et al.* (2016) Cellularly active N-hydroxyurea FEN1 inhibitors block substrate entry to the active site. *Nature chemical biology*, **12**, 815-821.
41. Zhang, F., Wang, Y., Wang, L., Luo, X., Huang, K., Wang, C., Du, M., Liu, F., Luo, T., Huang, D. *et al.* (2013) Poly(ADP-ribose) polymerase 1 is a key regulator of estrogen receptor alpha-dependent gene transcription. *The Journal of biological chemistry*, **288**, 11348-11357.
42. Lee, H.S., Park, J.H., Kim, S.J., Kwon, S.J. and Kwon, J. (2010) A cooperative activation loop among SWI/SNF, gamma-H2AX and H3 acetylation for DNA double-strand break repair. *The EMBO journal*, **29**, 1434-1445.
43. Nawaz, Z., Lonard, D.M., Dennis, A.P., Smith, C.L. and O'Malley, B.W. (1999) Proteasome-dependent degradation of the human estrogen receptor. *Proc Natl Acad Sci U S A*, **96**, 1858-1862.
44. Robinson, D.R., Wu, Y.M., Vats, P., Su, F., Lonigro, R.J., Cao, X., Kalyana-Sundaram, S., Wang, R., Ning, Y., Hodges, L. *et al.* (2013) Activating ESR1 mutations in hormone-resistant metastatic breast cancer. *Nature genetics*, **45**, 1446-1451.
45. Fan, M., Yan, P.S., Hartman-Frey, C., Chen, L., Paik, H., Oyer, S.L., Salisbury, J.D., Cheng, A.S., Li, L., Abbosh, P.H. *et al.* (2006) Diverse gene expression and DNA methylation profiles correlate with differential adaptation of breast cancer cells to the antiestrogens tamoxifen and fulvestrant. *Cancer Res*, **66**, 11954-11966.
46. Knowlden, J.M., Hutcheson, I.R., Jones, H.E., Madden, T., Gee, J.M., Harper, M.E., Barrow, D., Wakeling, A.E. and Nicholson, R.I. (2003) Elevated levels of epidermal growth factor receptor/c-erbB2 heterodimers mediate an autocrine growth regulatory pathway in tamoxifen-resistant MCF-7 cells. *Endocrinology*, **144**, 1032-1044.
47. Dai, X., Li, T., Bai, Z., Yang, Y., Liu, X., Zhan, J. and Shi, B. (2015) Breast cancer intrinsic subtype classification, clinical use and future trends. *Am J Cancer Res*, **5**, 2929-2943.
48. DiRenzo, J., Shang, Y., Phelan, M., Sif, S., Myers, M., Kingston, R. and Brown, M. (2000) BRG-1 is recruited to estrogen-responsive promoters and cooperates with factors involved in histone acetylation. *Molecular and cellular biology*, **20**, 7541-7549.

49. Callige, M. and Richard-Foy, H. (2006) Ligand-induced estrogen receptor alpha degradation by the proteasome: new actors? *Nucl Recept Signal*, **4**, e004.
50. Tecalco-Cruz, A.C. and Ramirez-Jarquin, J.O. (2017) Mechanisms that Increase Stability of Estrogen Receptor Alpha in Breast Cancer. *Clin Breast Cancer*, **17**, 1-10.
51. Maggi, A. (2011) Liganded and unliganded activation of estrogen receptor and hormone replacement therapies. *Biochim Biophys Acta*, **1812**, 1054-1060.
52. He, L., Zhang, Y., Sun, H., Jiang, F., Yang, H., Wu, H., Zhou, T., Hu, S., Kathera, C.S., Wang, X. *et al.* (2016) Targeting DNA Flap Endonuclease 1 to Impede Breast Cancer Progression. *EBioMedicine*.
53. Panda, H., Jaiswal, A.S., Corsino, P.E., Armas, M.L., Law, B.K. and Narayan, S. (2009) Amino acid Asp181 of 5'-flap endonuclease 1 is a useful target for chemotherapeutic development. *Biochemistry*, **48**, 9952-9958.
54. McManus, K.J., Barrett, I.J., Nouhi, Y. and Hieter, P. (2009) Specific synthetic lethal killing of RAD54B-deficient human colorectal cancer cells by FEN1 silencing. *Proc Natl Acad Sci U S A*, **106**, 3276-3281.
55. Klaeger, S., Heinzlmeir, S., Wilhelm, M., Polzer, H., Vick, B., Koenig, P.A., Reinecke, M., Ruprecht, B., Petzoldt, S., Meng, C. *et al.* (2017) The target landscape of clinical kinase drugs. *Science (New York, N.Y.)*, **358**.

Figure legends

Figure 1. FEN1 levels as predictive marker for tamoxifen response of breast cancer patients.

(A) Computational refinement of 111-gene classifier towards 4-gene classifier of FEN1, MCM2, HBP1 and STARD13. PAM and Lasso-penalized logistic regression was performed to determine the minimum number of genes without affecting performance. (Left) Recurrence-Free Survival (RFS) of patients categorized according to 111-gene classifier. Cox regression is shown. (Middle) Step-wise minimization of the 111-genes with corresponding average area under the curve (AUC) in two cohorts. (Right) RFS of patients categorized according to 4-gene classifier. Cox regression is shown. See also Sup Fig S1A

(B) Three representative IHC tumor cores, staining negative (0%), intermediate (50%) or entirely positive (100%) for FEN1. Scale bar is 100 μm.

(C) Scatterplot showing FEN1 mRNA levels (X-axis) related to FEN1 protein expression (% tumor cells, Y-axis), from the same tumor samples. Dotted line indicates trend line. Pearson correlation coefficient = 0.58.

(D) Bar graph showing the individual IHC-scores for all tumor samples. Tumors were stratified in "Low" (IHC-score ≤ 36%) or "High" (IHC-score > 36%) FEN1.

(E) Distant Metastasis-Free Survival (DMFS) of tamoxifen-treated patients categorized according to FEN1 mRNA levels. Log-rank and Cox regression is shown. See also Sup table S1.

(F) As in E, but now patients were categorized according to FEN1 IHC-score.

(G) Randomized clinical trial: RFS of patients stratified by ERα-status and categorized according to FEN1 IHC-score. Log-rank and Cox regression is shown. See also Sup table S1 and Sup Fig S1B.

(H) As in G, but now patients were stratified for adjuvant therapy (none or tamoxifen) and categorized according to FEN1 IHC-score. See also Sup table S1.

(I) As in G, but now patients were stratified for FEN1 IHC-score and categorized according to adjuvant therapy (none or tamoxifen). See also Sup table S1.

Figure 2. FEN interacts with ERα and dictates ERα-chromatin interactions and complex formation.

(A) Co-immunoprecipitation analyses demonstrate E2-induced ERα/FEN1 interactions. Protein levels were determined for ERα, FEN1, SRC3 and negative control Lamin A/C. Cells were treated with (+) or without (-) E2 before immunoprecipitation of ERα or IgG. Shown is an example of two biological replicates.

(B) Genome browser snapshot at the XBP1 locus, illustrating FOXA1 (green) and ERα (red) binding events for siFEN1 and control. Genomic coordinates and tag count are indicated. See also Sup Fig S2A,B,C.

(C) (left) Heatmap visualizing binding events of FOXA1 (green) and ERα (red) at ERα binding sites after FEN1 knockdown. All binding events are vertically aligned and centered on the ERα peak, with a 10 kb window. Peaks were sorted on ERα intensity. See also Sup Fig S2A,B,C. (right) Normalized tag counts of FOXA1 and ERα p300 are plotted, showing average signal intensity within a 10kb window.

(D) ERα binding motif analysis. SeqPos was used to identify binding motifs at all ERα binding sites (siControl) and motifs at sites no longer identified in siFEN1.

(E) Genomic distribution of the same set of ERα bindings sites decribed in D.

(F) As in C but now binding events of Formaldehyde-Assisted Isolation of Regulatory Elements sequencing (FAIRE-seq) are visualized. Shown is an example of two biological replicates.

Figure 3. FEN1 impacts ERα-mediated transcription and proliferation.

(A) Heatmap of the differentially expressed genes in E2 vs. vehicle treatment. Depicted are four biological replicates of siControl (grey bar) and siFEN1 (blue bar) cells treated with vehicle or E2.

(B) As in A, but now the differentially expressed genes in siFEN1 vs. aiControl are depicted.

(C) As in A, but now genes differentially expressed in both conditions are depicted.

(D) GSEA for Hallmark Estrogen Response Late genes. Shown is ranking metric using the log2FC*-log10pval. See also Sup Fig S3A.

(E) Relative cell proliferation (Y-axis) over time (X-axis) of MCF-7 cells treated with vehicle, E2, tamoxifen or fulvestrant. Cells were transfected with control siRNA (blue) or siFEN1 (red). Relative growth was normalized over the number of cells at timepoint zero. Shown is a representative experiment of three biological replicates. N=6 with mean ± SD with Students T-test at last time point. See also Sup Fig S3B,C.

(F) Relative cell proliferation of MCF-7 cells treated with vehicle, E2, tamoxifen or Fulvestrant. Cells were transfected with exogenous FEN1 (green) or GFP control (blue. Cell growth was normalized over GFP control after 150 hours of growth. Shown is a representative experiment of three biological replicates. N=6 with mean ± SD.

(G) As in E, but now MDA-MB-231 and CAL120 ERα-negative cells were grown in full medium. FEN1 and actin protein levels as assessed by western blot are depicted. Shown are representative experiments of two biological replicates. N=6 with mean ± SD.

Figure 4. FEN1 inhibitor screen and the role of FEN1 in ERα-activity.

(A) Fluorescence based assay used to assess flap-cleaving by FEN1. A double-stranded DNA flap substrate containing two tags, a fluorophore-donor (6-TAMRA) and a fluorophore-quencher (BHQ2), is exposed to FEN1 protein in the presence or absence of small-molecule compounds. Upon flap-cleavage the DNA product containing the fluorophore is released, resulting in measurable fluorescence signal.

(B) Concentration response profile of the 2,485 compounds found active as FEN1 inhibitors, identifying MLS002701801 (FENi#2) (purple dot) as our top hit. For each compound

the concentration (log) and the percentage of altered FEN1 enzyme activity is depicted. See also Sup Table S3 and Sup Fig S4A,B,C.

(C) Heatmap visualizing ranked binding events of ERα (red), PARP1 (dark cyan) and XRCC1 (purple) at ERα binding sites. Hormone-deprived cells where treated with E2 for 10 (ERα and XRCC1) or 30 minutes (PARP1). All binding events at ERα bound regions after 10 minutes of E2 were analyzed, vertically aligned and centered at the center of the peak, with a 10kb window. See also Sup Fig S4D.

(D) As in C but now binding events of ERα (red) and γH2AX (blue) at ERα binding sites, under vehicle or E2 conditions are visualized. Peaks were sorted on ERα intensity. See also Sup Fig S4E,F.

(E) Induction of γH2AX-foci by E2 stimulation as visualized through immunofluorescence. Hormone-deprived cells where treated with ethanol or E2 for 15 minutes, with or without FEN1 inhibitor. Shown is a representative cell stained for γH2AX (green). To-Pro-3-iodide was used to visualize the nucleus (blue). Scale bar indicates 2μm.

(F) The average number of γH2AX-foci per cell as quantified in 500 cells. Shown is a representative experiment of two biological replicates. N=500 with mean ± SD. See also Sup Fig S4G.

(G) (Upper left) Heatmap visualizing ranked binding events of ERα (red) at ERα sites. Hormone-deprived cells where pretreated with a vehicle or FEN1 inhibitor and subsequently stimulated with E2 for 10 minutes. All binding events at ERα sites after 10 minutes of E2 were analyzed, vertically aligned and centered at the center of the peak, with a 10kb window. Normalized tag counts are plotted, showing average signal intensity. (Upper right) As in Upper left but now ERα binding sites were analyzed for cells stimulated with E2 for 30

minutes. (Bottom left) As in Upper left but now PARP1 binding sites were analyzed for cells stimulated with E2 for 30 minutes. (Bottom right) As in Upper left but now BRG1 binding sites were analyzed for proliferating cells. See also Sup Fig S4H.

Figure 5. Small molecule-mediated inhibition of FEN1 blocks ERα action and prevents cell proliferation.

(A) ERα ChIP-qPCR analyses of hormone-deprived cells treated for 90 minutes with E2 using 5 minute intervals. Three positive regions for ERα-binding were assessed (TFF1, GREB1 and XBP1) and one known negative region (Neg control). Data are normalized over t=0. N=4 with mean ± SD.

(B) (Left) ERα ChIP-qPCR analyses of hormone-deprived cells pretreated with vehicle or FEN1 inhibitor prior to 30 minutes of E2 treatment. Signals are normalized over control genomics regions. Shown is a representative experiment of two biological replicates. N=4 with mean ± SD. (Right) Relative mRNA levels of RARA, XBP1 and TFF1 with or without FEN1 inhibitor. TBP and UBC were used as control. Shown is a representative experiment of two biological replicates. N=4 with mean ± SD.

(C) Colony formation analyses for breast cancer cell lines; MCF-7 and T47D (ERα+), MCF7-T and TAMR (tamoxifen resistant MCF-7 derivatives) and BT-20 and CAL-120 (ERα-). Cells were treated with increasing concentrations of FEN1 inhibitor in the presence or absence of tamoxifen. Representative experiment is shown of at least 4 biological replicates.

(D) Relative quantified crystal violet staining (OD_{560}) of colony formation assay depicted in (C). Shown are mean values of at least 4 biological experiments where all OD_{560} data were normalized to vehicle treated FBS. Error bars indicate SEM. See also Sup table S4.

(E) Ex vivo primary human ERα-positive tumor cultures in the presence or absence of 200 nM FEN1 inhibitor. Explants were fixed and stained for Ki67 and H&E. Shown are representative tumor regions for two patients with digital zoom in the lower right corner.

(F) Indication of the percentage of Ki67 positive tumor cells in tumor explants cultured in the presence or absence of FEN1 inhibitor. Paired Students T-test was used to assess the difference between treatment groups. See also Sup Fig S5D.

Figure 1

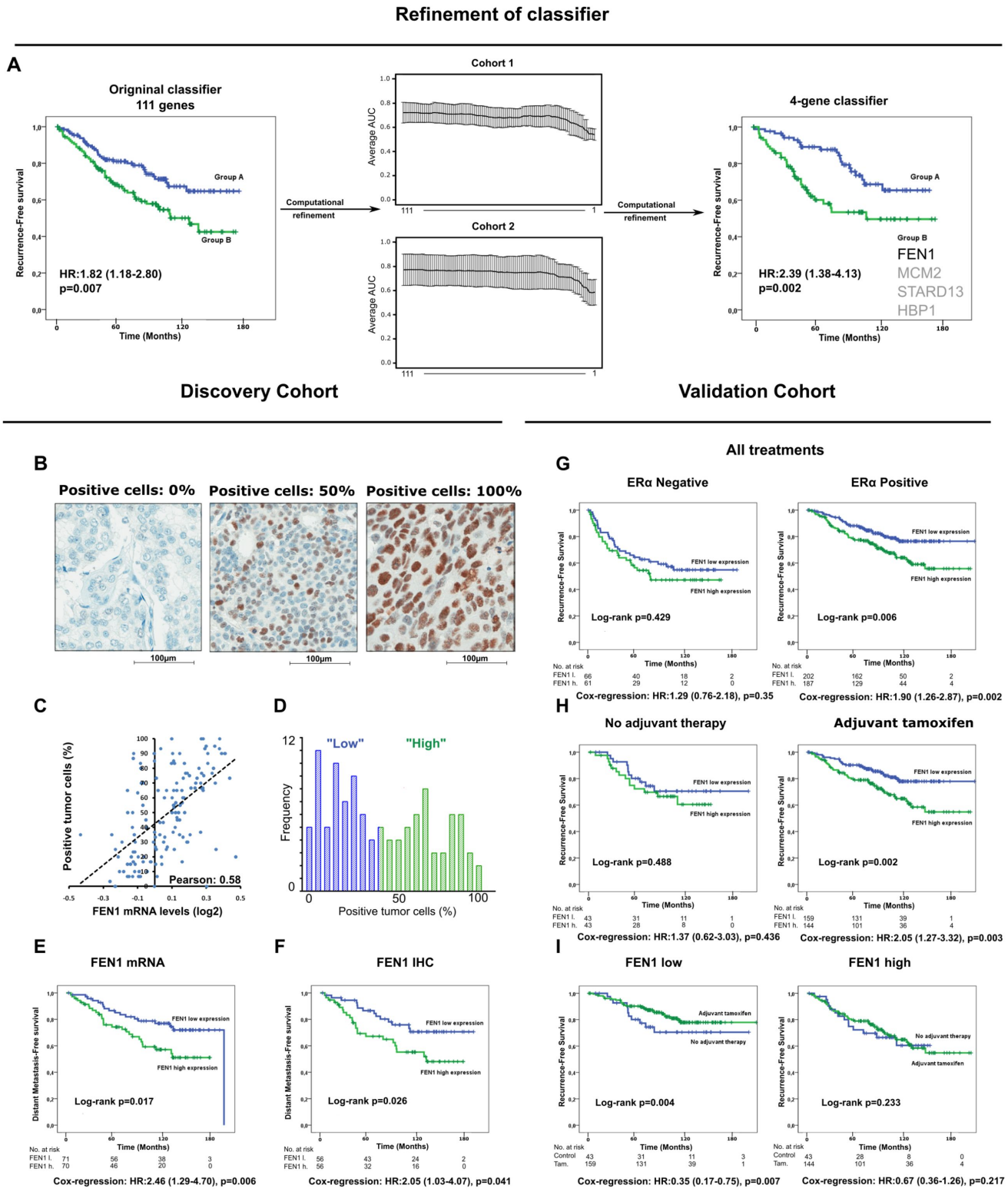
Refinement of classifier
A
Origninal classifier
111 genes
Recurrence-Free survival
Group A
Group B
HR:1.82 (1.18-2.80)
p=0.007
Time (Months)
Computational refinement
Cohort 1
Cohort 2
Average AUC
111
1
Computational refinement
4-gene classifier
HR:2.39 (1.38-4.13)
p=0.002
FEN1
MCM2
STARD13
HBP1
Discovery Cohort
Validation Cohort
B
Positive cells: 0%
Positive cells: 50%
Positive cells: 100%
100µm
C
Positive tumor cells (%)
Pearson: 0.58
FEN1 mRNA levels (log2)
D
"Low"
"High"
Frequency
Positive tumor cells (%)
E
FEN1 mRNA
Distant Metastasis-Free survival
FEN1 low expression
FEN1 high expression
Log-rank p=0.017
No. at risk
FEN1 l. 71 56 38 3
FEN1 h. 70 46 20 0
Cox-regression: HR:2.46 (1.29-4.70), p=0.006
F
FEN1 IHC
Log-rank p=0.026
No. at risk
FEN1 l. 56 43 24 2
FEN1 h. 56 32 16 0
Cox-regression: HR:2.05 (1.03-4.07), p=0.041
G
All treatments
ERα Negative
ERα Positive
Log-rank p=0.429
Log-rank p=0.006
No. at risk
FEN1 l. 66 40 18 2
FEN1 h. 61 29 12 0
Cox-regression: HR:1.29 (0.76-2.18), p=0.35
No. at risk
FEN1 l. 202 162 50 2
FEN1 h. 187 129 44 4
Cox-regression: HR:1.90 (1.26-2.87), p=0.002
H
No adjuvant therapy
Adjuvant tamoxifen
Log-rank p=0.488
Log-rank p=0.002
No. at risk
FEN1 l. 43 31 11 1
FEN1 h. 43 28 8 0
Cox-regression: HR:1.37 (0.62-3.03), p=0.436
No. at risk
FEN1 l. 159 131 39 1
FEN1 h. 144 101 36 4
Cox-regression: HR:2.05 (1.27-3.32), p=0.003
I
FEN1 low
FEN1 high
Adjuvant tamoxifen
No adjuvant therapy
Log-rank p=0.004
Log-rank p=0.233
No. at risk
Control 43 31 11 3
Tam. 159 131 39 1
Cox-regression: HR:0.35 (0.17-0.75), p=0.007
No. at risk
Control 43 28 8 0
Tam. 144 101 36 4
Cox-regression: HR:0.67 (0.36-1.26), p=0.217

Figure 2

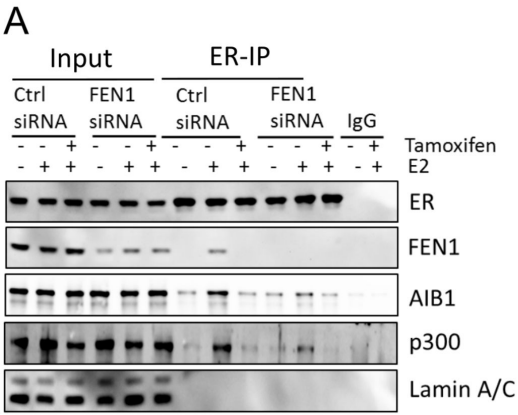
A
Input
ER-IP
Ctrl siRNA
FEN1 siRNA
Ctrl siRNA
FEN1 siRNA
IgG
Tamoxifen
E2
ER
FEN1
AIB1
p300
Lamin A/C

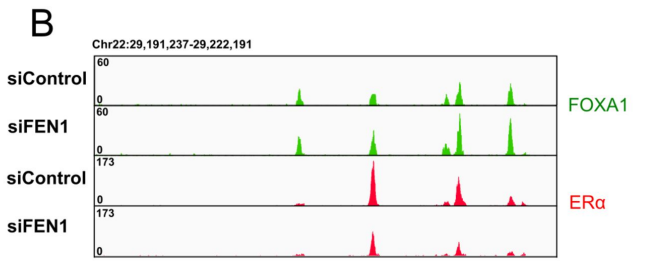
B
Chr22:29,191,237-29,222,191
siControl
siFEN1
siControl
siFEN1
FOXA1
ERα

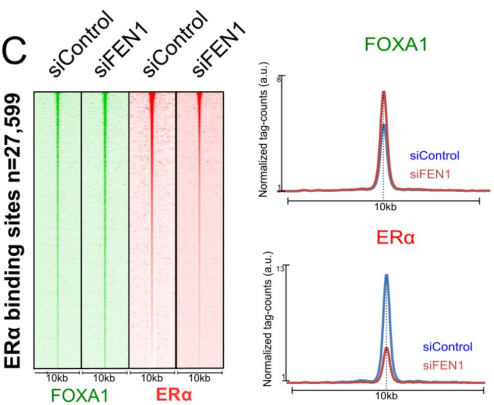
C
siControl
siFEN1
siControl
siFEN1
ERα binding sites n=27,599
FOXA1
ERα
Normalized tag-counts (a.u.)
siControl
siFEN1
10kb

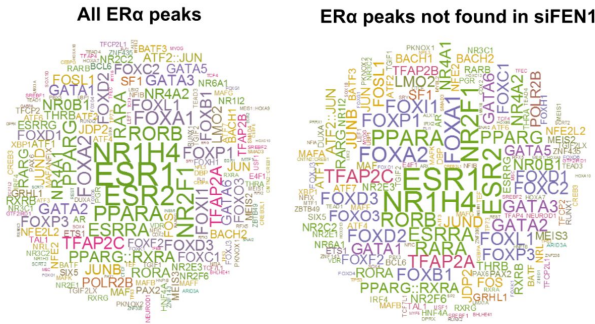
D
All ERα peaks
ERα peaks not found in siFEN1

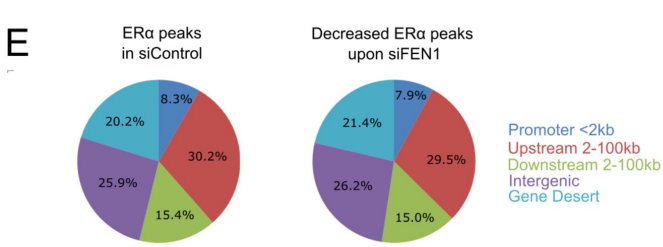
E
ERα peaks in siControl
Decreased ERα peaks upon siFEN1
8.3%
30.2%
15.4%
25.9%
20.2%
7.9%
29.5%
15.0%
26.2%
21.4%
Promoter <2kb
Upstream 2-100kb
Downstream 2-100kb
Intergenic
Gene Desert

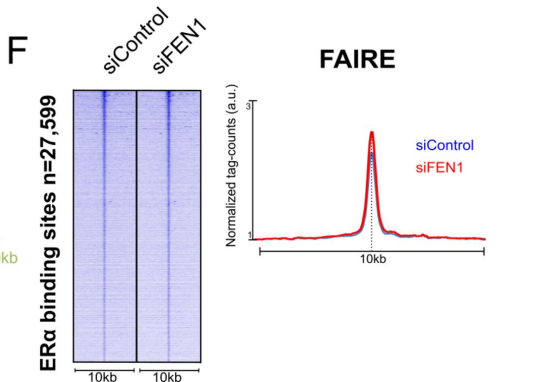
F
siControl
siFEN1
FAIRE
ERα binding sites n=27,599
Normalized tag-counts (a.u.)
siControl
siFEN1
10kb

Figure 3

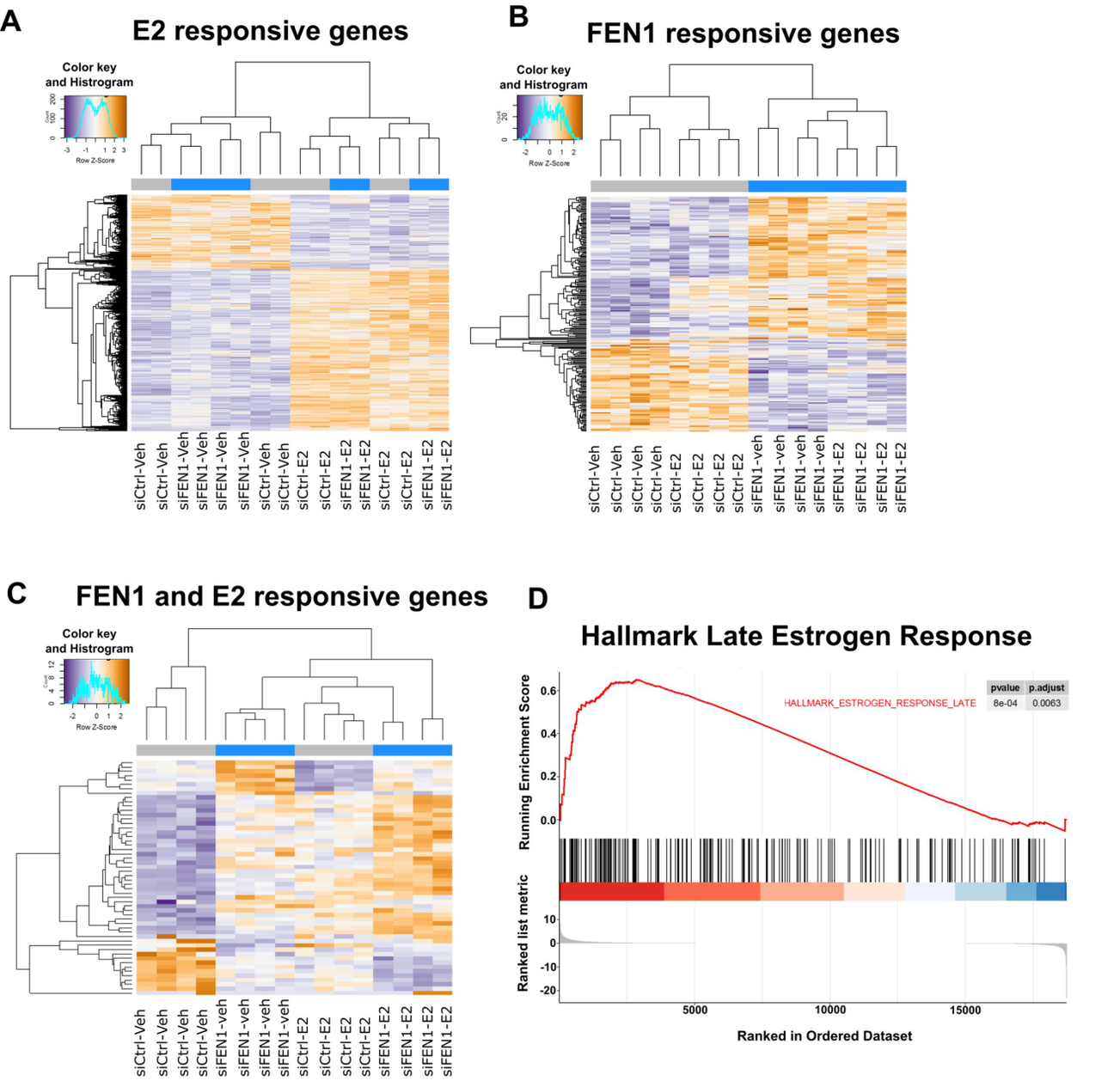

Cell proliferation

FEN1 knockdown

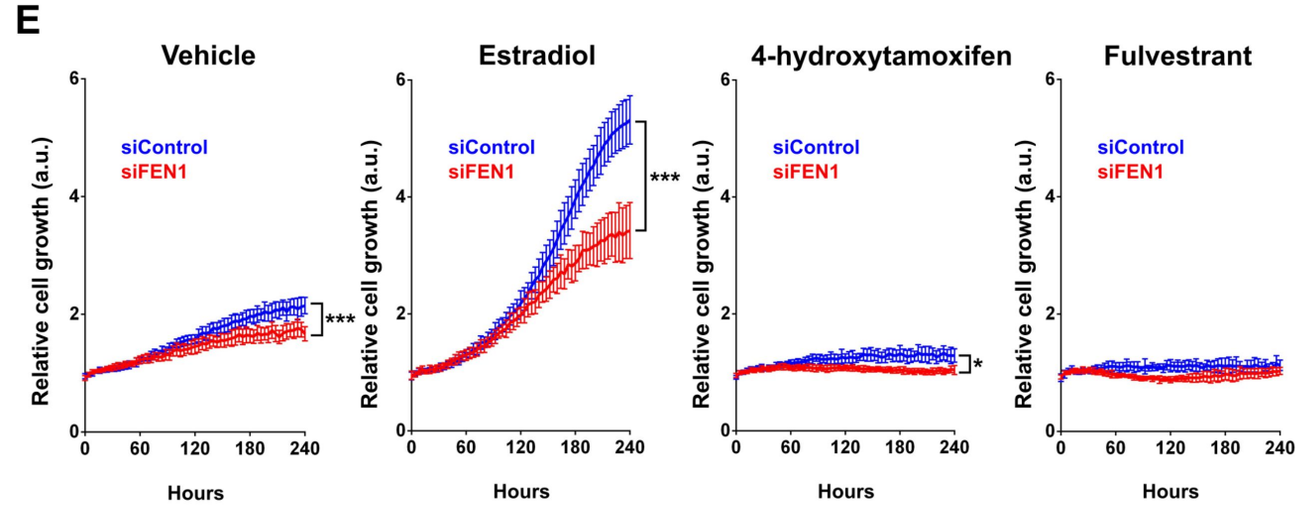

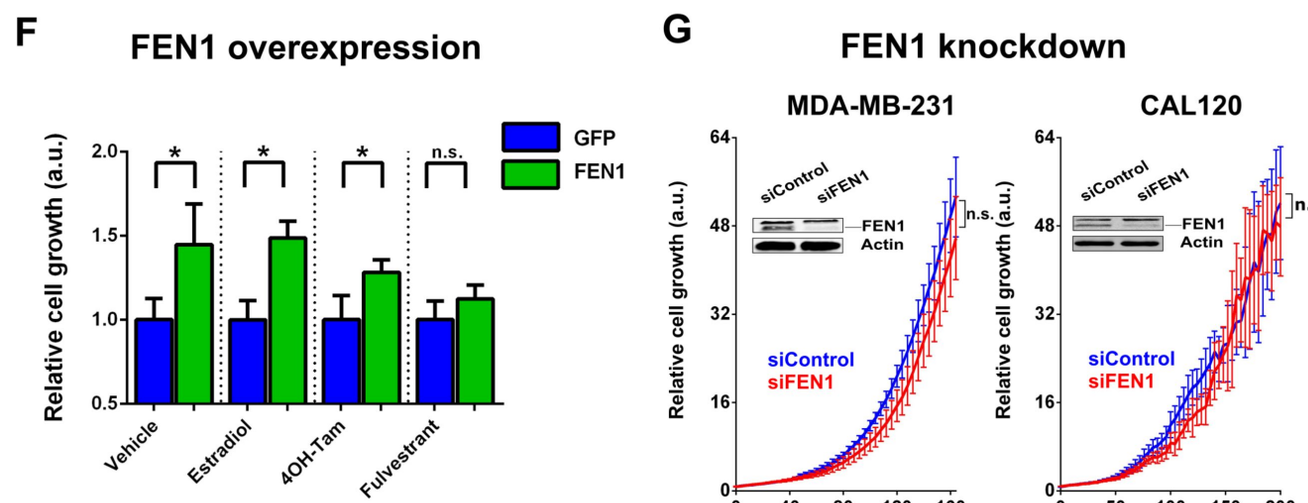

Figure 4

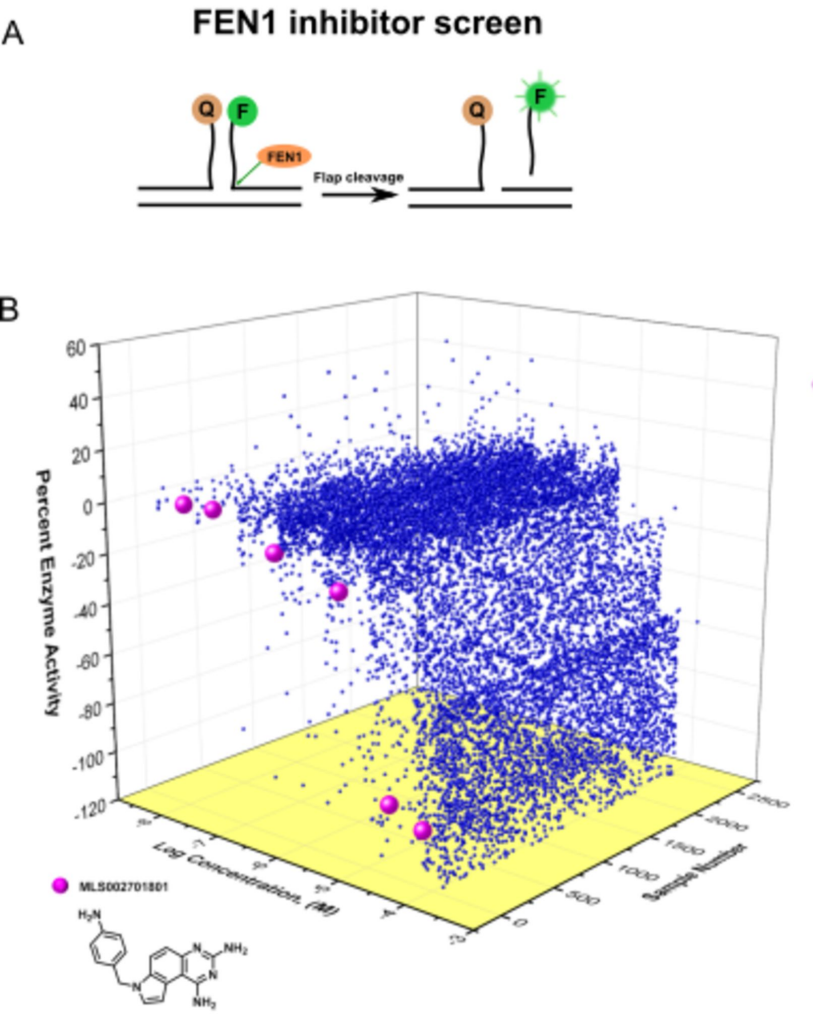
A
FEN1 inhibitor screen
Q
F
FEN1
Flap cleavage
B
Percent Enzyme Activity
Log Concentration, (M)
Sample Number
MLS002701801

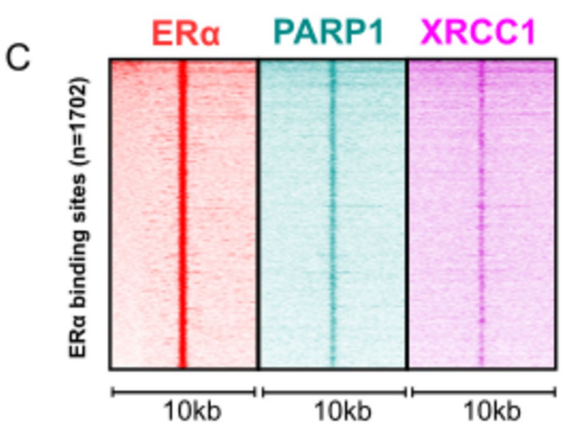
C
ERα
PARP1
XRCC1
ERα binding sites (n=1702)
10kb
10kb
10kb

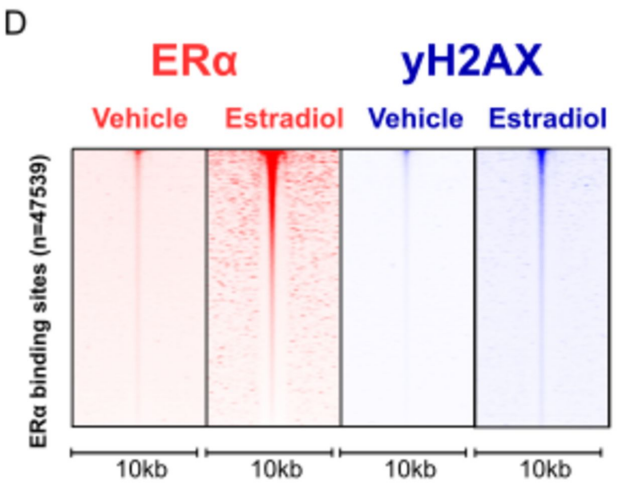
D
ERα
yH2AX
Vehicle
Estradiol
Vehicle
Estradiol
ERα binding sites (n=47539)
10kb
10kb
10kb
10kb

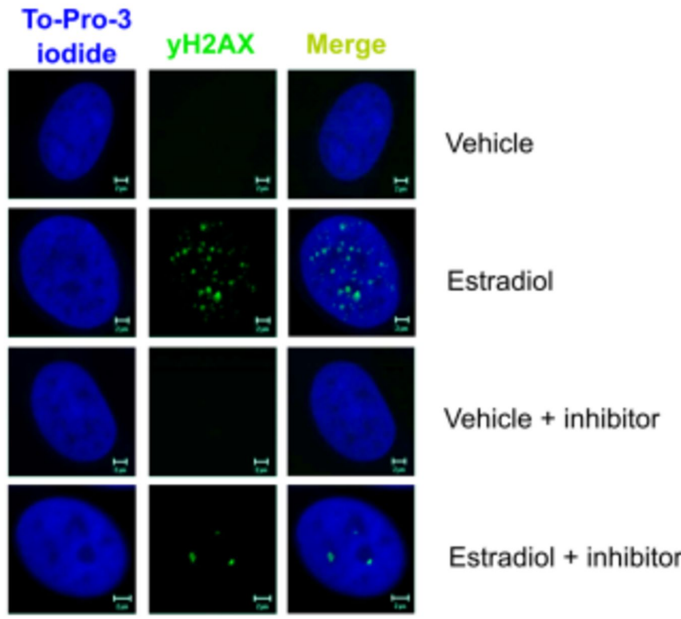
E
To-Pro-3 iodide
yH2AX
Merge
Vehicle
Estradiol
Vehicle + inhibitor
Estradiol + inhibitor

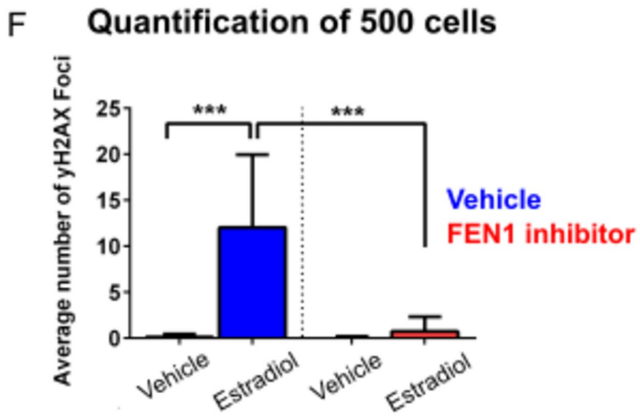
F
Quantification of 500 cells
Average number of yH2AX Foci
***
***
Vehicle
FEN1 inhibitor
Vehicle
Estradiol
Vehicle
Estradiol

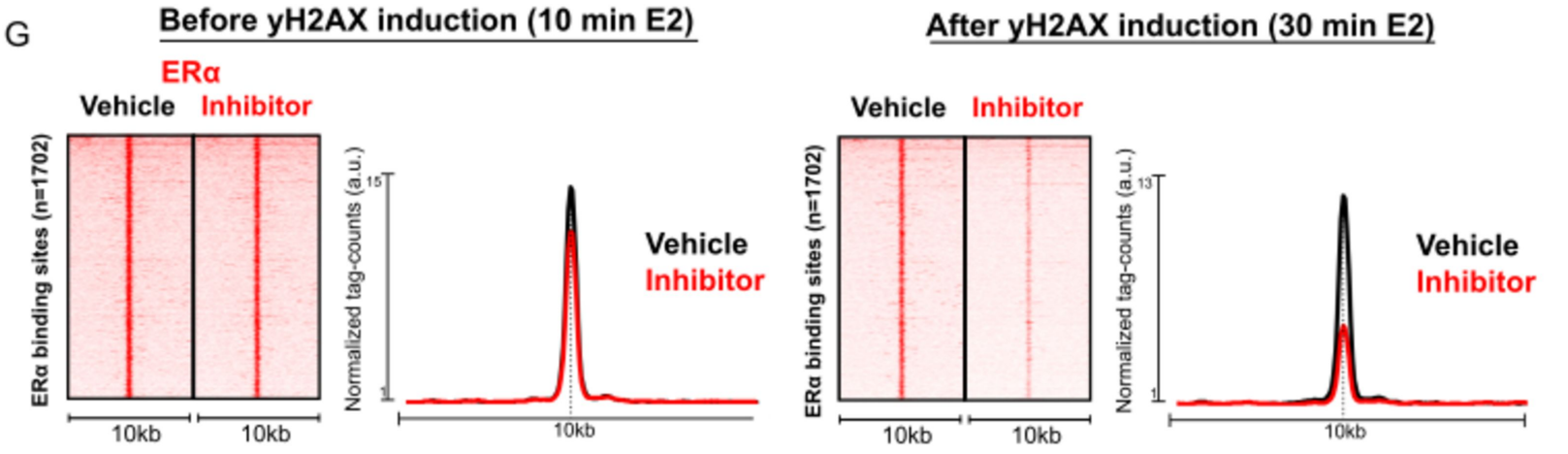
G
Before yH2AX induction (10 min E2)
After yH2AX induction (30 min E2)
ERα
Vehicle
Inhibitor
ERα binding sites (n=1702)
Normalized tag-counts (a.u.)
Vehicle
Inhibitor
10kb
30 min E2
PARP1
Proliferating
BRG1
ERα binding sites (top 10,000)

Figure 5

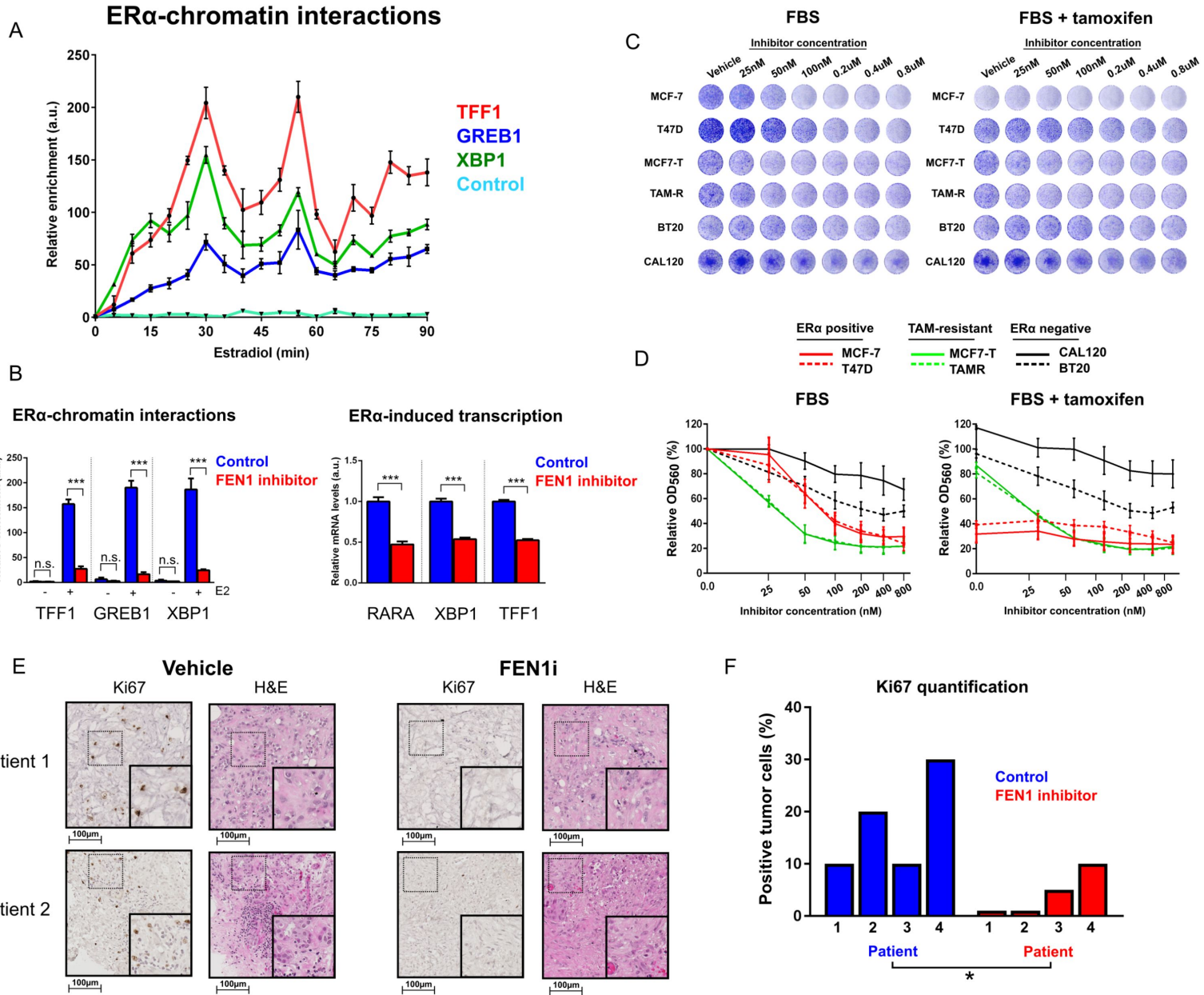
A
ERα-chromatin interactions
Relative enrichment (a.u.)
Estradiol (min)
TFF1
GREB1
XBP1
Control
B
ERα-chromatin interactions
ERα-induced transcription
Relative enrichment (a.u.)
Relative mRNA levels (a.u.)
Control
FEN1 inhibitor
n.s.
***
E2
TFF1
GREB1
XBP1
RARA
XBP1
TFF1
C
FBS
FBS + tamoxifen
Inhibitor concentration
Vehicle
25nM
50nM
100nM
0.2uM
0.4uM
0.8uM
MCF-7
T47D
MCF7-T
TAM-R
BT20
CAL120
D
ERα positive
MCF-7
T47D
TAM-resistant
MCF7-T
TAMR
ERα negative
CAL120
BT20
FBS
FBS + tamoxifen
Relative OD560 (%)
Inhibitor concentration (nM)
E
Vehicle
FEN1i
Ki67
H&E
Patient 1
Patient 2
100μm
F
Ki67 quantification
Positive tumor cells (%)
Control
FEN1 inhibitor
Patient
Patient
*